

## Measurement of Respiration Rate and Depth Through Difference in Temperature Between Skin Surface and Nostril by Using Thermal Image

Hieyong Jeong<sup>a</sup>, Yutaka Matsuura<sup>b</sup>, and Yuko Ohno<sup>a, c</sup>

<sup>a</sup> Department of Robotics & Design for Innovative Healthcare, Osaka University, Suita, Osaka, Japan,

<sup>b</sup> Graduate School of Dentistry, Osaka University, Suita, Osaka, Japan,

<sup>c</sup> Division of Health Sciences, Osaka University, Suita, Osaka, Japan.

### Abstract

The purpose of the present study was to propose a method to measure a respiration rate (RR) and depth at once through difference in temperature between the skin surface and nostril by using a thermal image. Although there have been a lot of devices for contact RR monitoring, it was considered that the subjects could be inconvenienced by having the sensing device in contact with their body. Our algorithm enabled us to make a breathing periodic function (BPF) under the non-contact and non-invasive condition through temperature differences near the nostril during the breath. As a result, it was proved that our proposed method was able to classify differences in breathing pattern between normal, deep, and shallow breath ( $P < 0.001$ ). These results lead us to conclude that the RR and depth is simultaneously measured by the proposed algorithm of BPF without any contact or invasive procedure.

### Keywords:

Thermography; Respiratory Insufficiency; Respiratory Rate.

### Introduction

Respiratory failure is one of the most common reasons for admission to the intensive care unit (ICU) and a common comorbidity in patients admitted for acute care [1]. What's more, it's the leading cause of death from pneumonia and chronic obstructive pulmonary disease (COPD) in the United States. Patients with impending respiratory failure typically develop shortness of breath and mental-status changes, which may present as anxiety, tachypnea, and decreased peripheral oxygen saturation (SpO<sub>2</sub>) despite increasing amounts of supplemental oxygen [2], [3]. It is possible to assess the patient's tissue oxygenation status regularly when the change of respiratory status is detected in the early stage. It follows that measuring the breath of the patient is important in the clinical environment.

The intensity of the care provided in the ICU requires many monitoring devices [4]. The ventilator, or respirator, is a breathing machine that helps patients breathe when they are too ill to breathe on their own. When signs and symptoms of respiratory failure are clearly strong, it is possible to use the ventilator at the appropriate time. However, when there are few signs and symptoms of respiratory failure, patients should be checked on a regular basis because symptoms can become suddenly or progressively worse. The current level of regular monitoring depends on the visual monitoring or stethoscope of caregivers, or the measurement of SpO<sub>2</sub> practically without any direct measurement of breath. In chronic respiratory failure, the

only consistent clinical indicator is protracted shortness of breath [5]. The ideal respiratory monitor will not only detect respiratory failure regardless of the cause, but also indicate the cause. Respiratory failure, which leads to severe medical problems, remains an important issue. However there seems to have been little to preclude our simple method of detecting the early stages of respiratory failure in the clinical environment.

Different respiratory monitoring methods measure different physiological variables [5]. According to our literature review, it is possible to divide existing non-invasive respiratory monitoring methods into three categories: detection of movement, volume and tissue composition; airflow sensing; and monitoring of blood gas concentrations.

#### Detection of movement, volume and tissue composition

Muscle activity causes variations in thorax volume and pressure that give rise to variations in the venous return of blood to the heart. Variations in thorax pressure cause variations in air volume within the lungs, which in turn result in variations in transthoracic impedance [6]. The methods included in this category are, besides transthoracic impedance monitoring [7], measurement of chest or abdominal circumference, electromyography, various motion detectors and photoplethysmography [8]. However, this method still struggles with measuring while patients have any movement.

#### Airflow sensing

It is possible to detect airflow because expiratory air is warmer, has higher humidity and contains more CO<sub>2</sub> than inspiratory air. Variations in these parameters can be used for indicating the respiratory rate. Even sound caused by the airflow can be used in a similar fashion. To be able to measure tidal volume, the airflow must be measured and integrated over time, or the volume itself must be measured. Both methods need a facemask or mouthpiece to collect the air. They are used in spirometers [9], but are not commonly used in monitoring devices [10]. The airflow sensing method has difficulties in measuring under the normal circumstances of daily life.

#### Monitoring of blood gas concentrations

Respiratory activity can be assessed indirectly by monitoring O<sub>2</sub> and CO<sub>2</sub> concentration in arterial blood using non-invasive methods. Oxygen saturation is available by pulse oximetry, end-tidal concentration of O<sub>2</sub> or CO<sub>2</sub> can be measured in expiratory air, and transcutaneous blood gas concentrations can be measured through the skin. When the end-tidal concentration of O<sub>2</sub> or CO<sub>2</sub> is measured, the relative change in concentration between expired and inhaled air for oxygen is less specific (roughly 21% for inhaled air and 16% for exhaled air) than that

for CO<sub>2</sub> (approximately 3% and nearly 0%, respectively) [3], [11], [12]. However, this method requires many contact points on the body of patient.

### Purpose

From a present survey of the literature, it can be concluded that the need for effective respiratory monitoring is well known to the clinical engineering community. The number of papers in which new devices are demonstrated is large and, in fact, much larger than the number of publications devoted to the evaluation of such devices, indicating that the exploratory phase is still not finished [5]. Few solutions, if any, have been subjected to scrutinised evaluation on the basis of clinical usefulness. The reason for this may be that most monitoring devices are not yet adapted to clinical conditions. Monitoring respiratory activity in clinical practice introduces a number of problems that do not exist in a well-controlled laboratory-like situation. It must be possible to obtain the respiration status without disturbing or harming the patient. The monitoring devices should allow natural, unprovoked patient behaviour, such as turning to the side, moving head, arms and legs, and breathing through either nose or mouth [10]. Focusing on these reasons, the present study aims for caregivers to measure breathing patterns through the method related to airflow sensing under the non-invasive and non-contact conditions.

The main purpose of the present study was therefore to propose a method of measuring respiration rate (RR) and depth at once through differences in temperature between the skin surface and the nostril by using thermal imaging. Because our algorithm enabled us to make a breathing periodic function (BPF) under the non-contact condition during the breath, the peak-peak time and the distance between maximum and minimum peaks of BPF were helpful for measuring both the RR and depth at once.

## Materials and Methods

### Materials

#### Human subjects and experimental procedure

Three human subjects (Age:  $29 \pm 4$  years old, Height:  $171.4 \pm 6.5$  cm, Body mass index (BMI):  $23.5 \pm 3.2$  kg/m<sup>2</sup>) were enrolled for the study at a local university. All of the subjects were informed of the nature of the experiments and consented for their data to be used in the study.

All thermal video recordings were carried out in parallel with a number of conventional contact-based respiration monitoring methods. This enabled a comparison to be carried out between the thermal imaging method and the conventional contact methods. The conventional contact respiration monitoring methods either measured the temperature variations between the inhaled and exhaled air using a nasal temperature probe, or measured SpO<sub>2</sub>. The thermal video recordings were performed with the subject resting comfortably in a chair. The recordings did not cause any form of distress to the subject. The recording room temperature was about 24°C and humidity was about 30%.

Fig. 1 shows an experimental procedure in the present study. It is considered that there are three types of breathing: normal, deep, and intentional shallow breathing. We would like to confirm whether the proposed method can measure the RR and depth at once or not, while it does not matter if the type of breathing pattern is changed. A subject performed the normal breathing during 30 s, and then did two times deep breathing

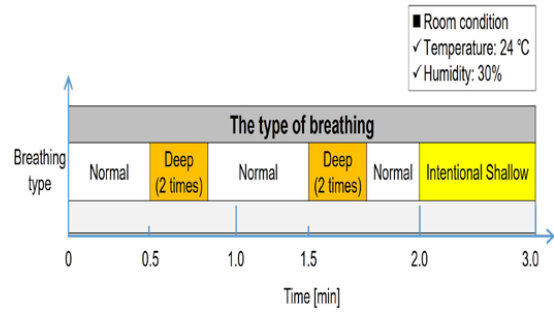


Figure 1 - Experimental procedure.

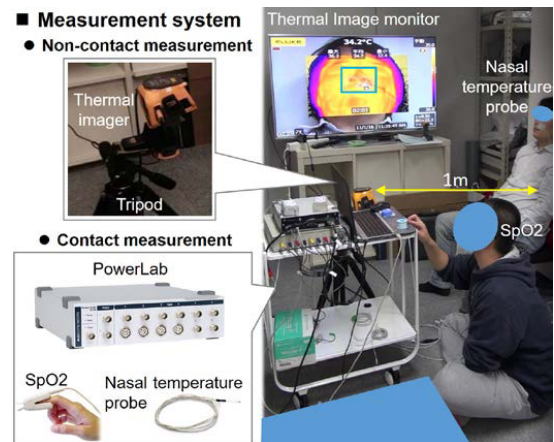


Figure 2 - Experimental system and environment.

within 1 min. Then the same performance was repeated one more time within an additional 1 min. Finally the subjects tried to perform the intentional shallow breathing during an additional 1 min, since for all subjects there were no problems with the experimental conditions. One subject performed three times under the same experimental conditions.

#### Experimental system

Fig. 2 shows an experimental system and environment. Apart from the 1.0 m distance, the thermal imager for the non-contact monitoring measures the ambient temperature of nostril and skin surface, and the nasal temperature probe for the contact monitoring also measures the ambient temperature around the nostril. The large monitor shows the respiration region of interest (ROI) which indicates the position of a rectangular boundary (blue rectangle) superimposed on a thermal image. A human pulse oximetry is used to measure blood oxygen saturation (SpO<sub>2</sub>) in the finger. A computer saves and analyzes all measured data with the calculation and analysis software of Matlab.

The Fluke thermal imager (Ti450 60 Hz) with MultiSharp™ Focus [13] delivers focus near and far in one image. Focus is one of the most important aspects of thermography, and an out of focus image can yield data that can lead to misdiagnosis. The Ti450 brings  $640 \times 480$  SuperResolution can show us even more detail with 4x the pixel data. An accuracy of temperature measurement was  $\pm 2\%$  (at 25°C nominal, whichever is greater). The thermal imager could calculate each maximum, minimum and average value from the ROI automatically. The feature extracted from this ROI enabled the breathing signal to be produced. The thermal imager was fixed

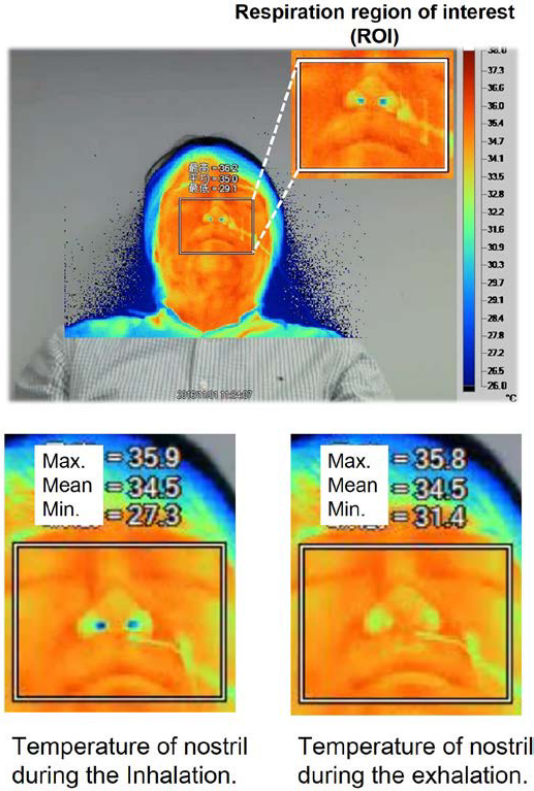


Figure 3 - The position of a rectangular boundary for the ROI superimposed on a thermal image (top) and differences in the temperature around nostril between inhalation and exhalation (bottom).

on a tripod in front of the subject at a distance of about one meter. Images were recorded at 9 frames per second (fps). The average respiration rate in an adult is about 15 cycles per minute (0.25 fps). Thus the image capture rate was sufficiently high. The duration of each recording was 3 min. This produced 1,620 thermal images per subject (1 × 9 × 60 × 3). The recorded images were processed off-line using the Matlab image processing tool box in the present study. The operations involved for processing the images are explained in the next sections.

The Nasal Temperature Probe (MLT415/AL) contains a small biomedical chip thermistor [14]. The thermistor is designed to operate from 0°C to 50°C. The nasal temperature probe is suitable for connection to the ML309 Thermistor Pod. The accuracy of the sensor was ± 0.15°C (if the temperature range was from 20°C to 35°C). The sampling frequency was set to 1 kHz.

Quick and easy to apply, these transducers (MLT321/MLT322 Human Pulse Oximetry) are ideal for spot checking and short-term continuous monitoring of SpO<sub>2</sub> [15]. The intensity of the transmitted light is measured and the ML320 Oximeter Pod produces a signal scaled to read in % SpO<sub>2</sub>. For this experiment, the finger clip was used. The accuracy of the sensor was ± 2% of full scale for adults using the finger clip sensor. The sampling frequency was set to 1 kHz. The SpO<sub>2</sub> data was especially useful for confirming whether a subject performed the proper shallow breathing or not as shown in Fig. 1.

### Methods

Fig. 3 (top) illustrates the position of a rectangular boundary for the ROI superimposed on a thermal image. To determine the respiration rate (RR) three phases are necessary: image acquisition, ROI tracking, and RR monitoring [16]. Image acquisition provides images from a thermal imager to ROI tracking and RR monitoring at a configuration rate. ROI tracking seeks the ROI in the current thermal image by providing a bounding box (BB). A BB consists of the coordinates (x, y) and the size (width w = 7 cm, height h = 5 cm) of the ROI. The size and position of BB can be changed by setting the thermal imager in advance. Although the BB coordinates are used to compute the position and orientation of the thermal imager, the BB is fixed to keep the ROI at the center of the image in the present study, as shown in Fig. 3 (top).

Finally, the RR can be calculated by the maximum and minimum temperature in the ROI. If the ROI is put to the m-by-n matrix of M<sub>BB</sub>, both the maximum and minimum temperature are decided as follows:

$$\begin{aligned} T_{max}(t) &= \max(M_{BB(m,n)}) \text{ [}^\circ\text{C]} \\ T_{min}(t) &= \min(M_{BB(m,n)}) \text{ [}^\circ\text{C]} \end{aligned} \tag{1}$$

where the character of m represents rows of matrix M<sub>BB</sub>, and the character of n represents columns. It is observed that mainly the maximum temperature in the ROI indicates the skin surface, and the minimum temperature in the ROI indicates differences in the temperature around the nostril during breathing as shown in Fig. 3 (bottom). Although the maximum temperature of skin surface in the ROI does not show much change during breathing, the minimum temperature of the nostril shows significant change between inhalation and exhalation. Thus the breathing periodic function (BPF) of the proposed algorithm is derived as follows:

$$BPF(t) = T_{max}(t) - T_{min}(t) \text{ [}^\circ\text{C]} \tag{2}$$

The maximum peak value of BPF indicates breathing. The breath corresponds to the phases of inhalation and exhalation. It is considered that differences in temperature between inhalation and exhalation indicates breathing. The number of peaks indicates the number of breaths, and the time gap between one peak and the next peak in the BPF indicates the RR. Generally the RR is measured in number of breaths per minute (BPM), and the RR normally lies between 12 and 16 BPM at rest for an adult. Thus the RR in this paper is calculated as follows:

$$RR_{(i)} = \frac{60}{\text{time gap}} \text{ [BPM]} \tag{3}$$

where the character of i represents the order of period of BPF.

Then, the distance gap between the maximum and minimum peaks indicates the depth of breathing. Thus the depth of breathing in this paper is calculated as follows:

$$Depth_{(in)} = \begin{cases} (peak_i^1 - peak_i^2), n = 1 \text{ if inhalation} \\ (peak_i^2 - peak_i^3), n = 2 \text{ if exhalation} \end{cases} \tag{4}$$

where the character of i represents the order of period of BPF. The meaning in n = 1 indicates the depth of breathing during the inhalation, and the meaning in n = 2 indicates the depth

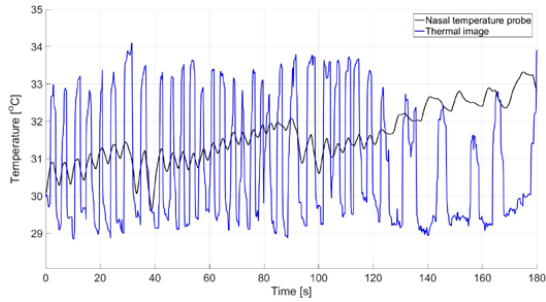


Figure 4 - Results of measured BPF by comparison with nasal temperature probe.

during the exhalation. It is considered that the distance gap of BPF means the relative depth of breathing. For example, the large difference in  $Depth_{i1}$  or  $Depth_{i2}$  by comparison with the normal breathing indicates deep breathing, and the small difference indicates shallow breathing.

Our proposed algorithm enables us to measure the RR and depth of breathing at once under the non-contact and non-invasive conditions by using the BPF of the thermal image as shown in equations (3) and (4). Furthermore, we would like to emphasize that it is possible to differentiate between inhalation and exhalation as shown in the equation (4).

## Results

### Results of measured BPF

It is necessary to understand the waveform of BPF which is used to measure the RR and depth of breathing. Figure 4 illustrates the results of measured BPF in comparison to measured data of the nasal temperature probe. The  $x$  axis indicates experimental time, and the  $y$  axis indicates temperature value. The black line represents the data of the nasal temperature probe, and the blue line represents those of BPF. The nasal temperature probe is regarded as the reference in the present study. In order to facilitate direct comparison between the two datasets, the initial value of BPF is added to the initial value of the nasal temperature probe. Because the initial value of BPF is about the lower value of 4.5°C before the addition of a baseline, it seems that it is difficult to compare differences between the two datasets directly. The increasing temperature value indicates the inhalation status, and the decreasing temperature indicates the exhalation status.

As a result, it was found that there were not significant differences in the period between the two different plots at all, although the type of breathing (normal, deep, and intentional shallow breathing) was changed according to the experimental procedure as shown in Fig. 1. Furthermore, although it seemed that there were big differences in maximum and minimum peaks between the two different data, it was no matter to extract featured points according to the different type of breathing.

The increasing slope of BPF after 2 min for the nasal temperature probe came from the abnormal weak inhalation and the influence of skin temperature on the measurement under the contact condition. However, because the proposed algorithm used the non-contact method, it was considered that the influence of the abnormal weak inhalation and skin temperature on the measurement was little.

Table 1 - Results of classification between the three different types of breathing.

No.	Index	The type of breathing		
		Normal	Deep	Intentional Shallow
■ Nasal temperature probe				
1	RR [BPM]	$15.86 \pm 2.17$	$10.51 \pm 2.24$	$6.59 \pm 2.47$
2	Depth in inhalation [°C]	$-0.39 \pm 0.14$	$-1.11 \pm 0.44$	$-0.43 \pm 0.24$
3	Depth in exhalation [°C]	$0.44 \pm 0.13$	$1.14 \pm 0.47$	$0.66 \pm 0.20$
■ Thermal image				
1	RR [BPM]	$15.99 \pm 3.36$	$10.42 \pm 2.47$	$6.61 \pm 2.35$
2	Depth in inhalation [°C]	$3.88 \pm 0.44$	$4.52 \pm 0.41$	$3.02 \pm 0.61$
3	Depth in exhalation [°C]	$-3.86 \pm 0.43$	$-4.59 \pm 0.44$	$-3.01 \pm 0.52$

### Results of classification between the different types of breathing

It is necessary to prove whether it is possible to distinguish between the different types of breathing in the present study or not, through the proposed method. Table 1 shows the results of classification between the three different types of breathing. According to the experimental procedure with the three different types of breathing (normal, deep, and intentional shallow breathing), all of the indices are analyzed.

For the RR, values of  $15.99 \pm 3.36$  BPM,  $10.42 \pm 2.47$  BPM, and  $6.61 \pm 2.35$  BPM for the thermal image under the condition of normal, deep, and shallow breathing were similar to those of  $15.86 \pm 2.17$  BPM,  $10.51 \pm 2.24$  BPM, and  $6.59 \pm 2.47$  BPM for the nasal temperature probe under the same condition. This points to a high accuracy for the proposed algorithm for the measurement of RR. It was easy to distinguish the difference in the RR between the three different types of breathing ( $P < 0.001$ ).

For the inhalation depth ( $Depth_{i1}$ ), although values of  $3.86 \pm 0.44^\circ\text{C}$ ,  $4.52 \pm 0.41^\circ\text{C}$ , and  $3.02 \pm 0.61^\circ\text{C}$  for the thermal under the condition of normal, deep, and shallow were different from those of  $-0.39 \pm 0.14^\circ\text{C}$ ,  $-1.11 \pm 0.44^\circ\text{C}$ , and  $-0.43 \pm 0.24^\circ\text{C}$  for the probe under the same condition, it was easy to distinguish between the three different types of breathing (normal vs. deep:  $P < 0.001$  and  $P < 0.001$ , normal vs. shallow:  $P < 0.001$  and  $P = 0.164$ , deep vs. shallow:  $P < 0.001$  and  $P < 0.001$ ) except for the case (normal vs. shallow:  $P = 0.164$  for the nasal temperature probe). As the possible explanation, it was considered that the increasing slope of BPF for the nasal temperature probe under the condition of shallow breathing as shown in Fig. 6 resulted in this problem. This may be why the weak inhalation under the condition of contact method resulted in the increasing slope of BPF due to the effect of skin surface temperature.

For the exhalation depth ( $Depth_{i2}$ ), although values of  $-3.86 \pm 0.43^\circ\text{C}$ ,  $-4.59 \pm 0.44^\circ\text{C}$ , and  $-3.01 \pm 0.52^\circ\text{C}$  for the thermal under the condition of normal, deep, and shallow were different from those of  $0.44 \pm 0.13^\circ\text{C}$ ,  $1.14 \pm 0.47^\circ\text{C}$ , and  $0.66 \pm 0.20^\circ\text{C}$  for the probe under the same condition, it was easy to distinguish between the three different types of breathing (normal vs. deep:  $P < 0.001$  and  $P < 0.001$ , normal vs. shallow:  $P < 0.001$  and  $P < 0.001$ , deep vs. shallow:  $P < 0.001$  and  $P = 0.001$ ).

As a result, it was proved that our proposed method was able to classify differences in the RR and depth between normal, deep, and shallow breathing through the non-contact and non-invasive method by using the thermal image with a meaningful statistical significance under the natural conditions of daily life. In addition, because the BPF for measuring the RR and depth was based on differences in the temperature between the skin

surface and nostril, we would like to emphasize that it was considered that there was no difference among individuals. That was the reason why all subjects had differences in temperature between the skin and nostril during the breathing. These were strong points for the proposed method.

## Conclusion

In this study, we demonstrated that the acquisition and analysis of the breathing signal are possible using thermal infrared imaging. The proposed algorithm, which measures the RR and depth of breathing through the BPF, is non-contact, non-invasive, and highly automated. This means that it can be safely employed to monitor patients in the clinical environment as well as at home for long periods of time.

The analysis of the experimental results indicates that the pattern of breathing is remarkably consistent for the same individual over time. Therefore, abnormalities in the individual patterns can be easily spotted. The feasibility of this new proposed algorithm is discussed for clinical studies.

## Acknowledgements

This project was funded by the Hirose International Scholarship Foundation.

We wish to thank the industrial partners involved with the Konoike Institute of Technology, Konoike Transport Co., Ltd. (Room K708, 7th Floor, 3-1, Ofuka-cho, Kita-ku, Osaka 530-0011, Japan), who helped us find this avenue of research to begin with. We thank Mr. Tianyi Wang, Mr. Takafumi Ohno, Mr. Hideto Imai, and Prof. Michiko Kido, from Osaka University for their analysis of the measured data and their generous comments on the analysis results.

## References

- [1] M. Fournier, Caring for patients in respiratory failure, *American Nurse Today* 9 (2014), 18-23.
- [2] K. Rehder and H. Michael Marsh, Respiratory Mechanics During Anesthesia and Mechanical Ventilation, *Handbook of Physiology, The Respiratory System, Mechanics of Breathing* (2011), 737-752.
- [3] A. Davies, A. G. H. Blakeley, C. Kidd, Human Physiology: The respiratory system, *Churhill Livingstone* (2001), 647-707.
- [4] G. S. Johnson, A Guide to ICU Equipment After Severe Brain Injury, *The Brain Injury Law Group* (Access date: 22 Nov 2016), <http://tblaw.com/icu-equipment.html>.
- [5] M. Folke, L. Cernerud, M. Ekström, and B. Hök, Critical review of non-invasive respiratory monitoring in medical care, *Medical & Biological Engineering & Computing* 41 (2003), 377-383.
- [6] B. H. Brown, R. H. Smallwood, D. C. Barber, P. V. Lawford, and D. R. Hose, MEDICAL PHYSICS AND BIOMEDICAL ENGINEERING, *IOP Publishing Ltd.* (1999), Chapter 17-18.
- [7] K. P. Cohen, W. M. Ladd, D. M. Beams, W. S. Sheers, R. G. Radwin, W. J. Tompkins, and J. G. Webster, Comparison of impedance and inductance ventilation sensors on adults during breathing, motion, and simulated airway obstruction, *IEEE Trans Biomed Eng* 44 (1997), 555-566.
- [8] L. Nilsson, A. Johansson, and S. Kalman, Monitoring of respiratory rate in postoperative care using a new photoplethysmographic technique, *J Clin Monit Comput* 16 (2000), 309-315.
- [9] W. Perez and M. J. Tobin, Separation of factors responsible for change in breathing pattern induced by instrumentation, *J Appl Physiol* 59 (1985), 1515-1520.
- [10] M. Folke, F. Granstedt, B. Hök, and H. Scheer, Comparative provocation test of respiratory monitoring methods, *J Clin Monit* 17 (2002), 97-103.
- [11] M. W. Jopling, P. D. Manheimer, and D. E. Bebout, Effects of severe motion on three pulse oximeters designed for use in motion, *Int J Intens Care* (2000), 177-179.
- [12] T. E. Loughnan, J. Monagle, J. M. Copland, P. Ranjan, and M. F. Chen, A comparison of carbon dioxide monitoring and oxygenation between

facemask and divided nasal cannula, *Anaesth Intens Care* 28 (2000), 151-154.

- [13] FLUKE, (Access date: 22 Nov 2016), <http://en-us.fluke.com/products/infrared-cameras/fluke-ti450-infrared-camera.html>.
- [14] AD Instruments, Nasal Temperature Probes, (Access date: 22 Nov 2016), <https://www.adinstruments.com/products/nasal-temperature-probes>.
- [15] AD Instruments, SpO<sub>2</sub> Clips, (Access date: 22 Nov 2016), <https://www.adinstruments.com/products/spo2-clips>.
- [16] R. Chauvin, M. Hamel, S. Briere, F. Ferland, F. Grondin, D. Letourneau, M. Tousignant, and F. Michaud, Contact-Free Respiration Rate Monitoring Using a Pan-Tilt Thermal Camera for Stationary Bike Telerehabilitation Sessions, *IEEE Systems Journal* 10 (2016), 1046-1055.
- [17] C. L. Deepika, A. Kandaswamy, and G. Pradeepa, An efficient method for detection of inspiration phase of respiration in thermal imaging, *Journal of Scientific & Industrial Research* 75 (2016), 40-44.
- [18] R. Murthy and I. Pavlidis, Noncontact measurement of breathing function, *IEEE Eng Med Biol Mag* 25 (2005), 57-67.
- [19] A. K. Heiman, K. T. Orlikowsky, and L. Steffen, Non-contact respiratory monitoring based on real-time IR-thermography, *Proc World Congr Med Phys Biomed Eng* 25 (2009), 1306-1309.

## Address for correspondence

Hieyong Jeong, PhD

Department of Robotics & Design for Innovative Healthcare,

Graduate School of Medicine, Osaka University

1-7 Yamadaoka, Suita, Osaka 565-0871, Japan

TEL: +81-6-6879-2614

E-mail: [h.jeong@sahs.med.osaka-u.ac.jp](mailto:h.jeong@sahs.med.osaka-u.ac.jp)